

UTRECHT UNIVERSITY

GRADUATE SCHOOL OF NATURAL SCIENCES

Institute for
Marine and Atmospheric
research Utrecht



Master of Science in Climate Physics

**SENSITIVITY OF THE AMAZON RAINFOREST
TO CLIMATE CHANGE**

First supervisor Dr. Anna von der Heydt
Second supervisor Prof. dr. ir. Henk Dijkstra
Daily supervisor Dr. René van Westen

Master thesis of
Edoardo Bellincioni
Student no. 4291873

Abstract

The stability of the Amazon rainforest against precipitation changes has been commonly studied by means of conceptual models, from which the existence of two equilibria (savanna and tree-covered) emerges. These conceptual models are based on large spatial and temporal averages of climatic variables. However, no final, comprehensive proof of bi-stability is available for the Amazon, but results are supported by a growing evidence for it. On the other hand, biome models coupled to atmospheric models better reproduce the temporal and spatial dynamics of the Amazon basin, at the cost of higher computational cost. In literature, the only available studies which make use of a coupled vegetation-atmospheric model to show multiple equilibria have a spatial resolution of $\sim 2^\circ$ ($\sim 220\text{km}$): too coarse to properly represent the local variations of the precipitation field, especially in a system (such as the Amazon) where precipitation is one of the main drivers of change. Here we used the results of a fully-coupled, fixed-vegetation climate model run under a yearly 1% pCO₂ increase with a spatial resolution of 0.25° ($\sim 28\text{km}$) and a temporal resolution of 3h to project the climatic variables (relevant for the Amazon) for end-of-century. We then fed an equilibrium biome model with the output of the climate model, ran sensitivity analyses of the biome model to different parameters, and framed the end-of-century projections among the simulated equilibrium states of the rainforest. Although substantial changes (-24% trees) in the biomes of the rainforest are projected for end-of-century, the lack of vegetation feedbacks in this setup prevented us from investigating any non-linear behaviour. Thus, we successfully implemented a simple evaporation advection scheme, which shows a coupled response of precipitation and biome variations, and suggests a stronger response between the rainforest to climate change if advection is included. This method paves the way for similar studies that could resolve non-linearities, exploiting state-of-the-art climate models and sophisticated biome models to explore spatially-resolved biome distributions with wider ranges of climate forcings.

Contents

1	Introduction	4
2	Methods and Models	8
2.1	Numerical Simulation of the Amazon climate	8
2.1.1	Data	8
2.1.2	Evaluation of Present-day and Future Climate	9
2.2	Biome model - BIOME4	11
3	Amazon climate modelling	14
3.1	Present day precipitation	14
3.2	End-of-century precipitation	17
4	Amazon vegetation modelling	19
4.1	Sensitivity to absolute warming/drying	19
4.2	Sensitivity to lengthening of the dry season	20
4.3	Sensitivity to strengthening of dry season	22
4.4	Sensitivity to CO ₂	23
4.5	BIOME4 with scaled input	24
4.6	Evaporation advection scheme	24
5	Discussion and Conclusion	29

6 Acknowledgements	32
7 Supplementary Figures	33
List of Figures	40
List of Tables	47
Bibliography	48

1. Introduction

The Amazon rainforest has been denoted as susceptible to abrupt changes in the future climate projections¹. It has been suggested that the present day Amazon region can exist in multiple equilibria, namely a tropical rainforest or a savanna state²³⁴⁵. The importance of a healthy Amazon rainforest in both the local and global climate is beyond any doubt: the Amazon rainforest is a major player in the global carbon cycle⁶⁷⁸, storing 100-200 PgC, which could be released in the atmosphere through forest destruction³; the rainforest itself is then responsible for the runoff of the homonymous river, which accounts for around 20% of the global freshwater input to the oceans⁸⁷, as well as being the major water source for local population sustainment and agriculture.

Among the climatic parameters that induce changes in the Amazon rainforest, the ones that received most attention – due to their greater relative importance – have been deforestation and changes in precipitation and CO₂ concentration^{3;4}. In this context, CO₂ shall be considered only as a direct driver, interacting with the evapotranspiration of the plants.

The sustainability of a forest biome in the Amazon basin is strictly linked to the evapotranspiration-induced rainfall⁵. About two thirds of the moisture that precipitates in the Amazon region has originated in the Atlantic Ocean⁷. When moisture reaches the region from the Atlantic, it gets uptaken and recycled. This mechanism is possible only in presence of a healthy tropical forest: savanna, cropland or pasture do not store enough water for evapotranspiration to self-sustain⁵. Evapotranspiration coming from deforested areas is reduced by at least 20%, and the available moisture for precipitation decreases consequently⁵, both locally and in westward cascade of evaporation and precipitation. Deforestation has been treated differently in literature. Cox et al.³ and Nobre et al.⁴ stated that it played a negligible role. Nobre et al.⁴ inferred that its role was bound to become negligible as the rate had decreased 80% over the period 2005-2015. However, more recent papers (such as Silva Junior et al.⁹) measured a strong

increase in the rate of deforestation in the years 2017-2020. As deforestation is only men-driven, its fate is mainly a political matter.

Amazonian precipitation seasonal variability is already significant^{4;7}. The Amazon sees a dry and a wet season alternating throughout the year. The length of the seasons (especially the dry one) is strongly influencing the resilience of the forest. Tropical biomes can sustain mild droughts⁷, but the climate-change driven lengthening of the dry season, or the possible decrease in average precipitation, may endanger the strengths of negative feedbacks: experimental studies demonstrated a physiological adaptation of the trees to the alternating wet-dry seasons, which failed when the forest was subject to extremely prolonged droughts (see Davidson et al.⁷); Hirota et al.² developed an idealised multiple equilibria model, where they connected the stability of the “tree-covered” equilibrium state to mean annual precipitation in the region: lowering the precipitation makes the model more prone to undergo a transition from a tree-covered state to a savanna state. Salazar and Nobre¹⁰ found that with a dry season longer than 4 months, a tropical rainforest is not sustainable.

In addition to that, the Atlantic and Pacific oceans play an important role on the precipitation in the Amazon⁶. Its link to El Niño Southern Oscillation (ENSO) is solid^{2;3;4;7;6}: during a El Niño phase, droughts happen in the Amazon; during a La Niña phase, floods happen. This is due to the altered East-West Walker circulation, that occurs as a consequence of the anomalous vertical motion over the Central Pacific induced by temperature anomalies over the equatorial Pacific⁶. Similarly, North Atlantic tropical sea surface temperature (SST) has been found to positively correlate with Amazon precipitation⁶. Harris et al.¹¹ connected the Atlantic meridional SST gradient to precipitation in the Amazon, although claiming it to be of less importance compared to Pacific zonal SST gradients (ENSO). In the case of the Atlantic, an anomalous meridional SST gradient induces a meridional shift of the Intertropical Convergence Zone (ITCZ), which is responsible for a significant part of the Amazonian precipitation⁶.

The increased CO₂ concentrations due to anthropogenic climate change tend to exacerbate the consequences of the physiological reaction of plants: stomatal closure as a consequence of high CO₂ concentrations may result in decreased transpiration and thus reduced evaporative cooling. This would be on top of higher temperatures coming from a CO₂-induced increased greenhouse effect.

A common approach to investigating the stability of the Amazon rainforest under climate change is by means of a conceptual model, which links relevant proxies of the rainforest health (such as net primary productivity *NPP*^{1;11;12;10;13}, tree cover fraction^{3;12;2}, vegetation carbon budget^{3;12}) to global climate indices

(such as Atlantic Tropical SST⁶, Atlantic meridional SST gradients¹¹, ENSO indices^{2;3;4;7;6}). This approach has been fruitful, in that it has suggested the existence of multiple equilibria and tipping points in the Amazon region. However, so far it has not been possible to study full transitions associated with the tipping in fully-coupled climate models. Moreover, the physical processes resulting in multiple equilibria of rainforest vegetation need to be validated with more sophisticated models including smaller scale dynamics and observations. Nonetheless, there has been some research making use of dynamic vegetation models, but these were coupled to spatially and temporally coarse GCMs^{14;15}.

Yet even recent General Circulation Models (GCMs) exhibit a persistent precipitation bias over the tropics (see Siongco et al.¹⁶ for CMIP5 models): Atlantic westerly wind biases induce SST biases, which in turn poorly modulate the seasonal cycle of precipitation¹⁶.

Simulations of the future climate in fully-coupled climate models consistently project a weakening of the Atlantic Meridional Overturning Circulation (AMOC). The AMOC strength affects the location of the ITCZ. A weaker AMOC affects meridional SST gradients, and in such circumstance the ITCZ is expected to shift southwards over the Atlantic Ocean¹⁷, altering the equatorial-tropical precipitation, which can directly affect the health of the Amazon rainforest. It has been shown that the accuracy of a model in simulating SST changes (and thus oceanic climate change, AMOC weakening and ITCZ shifts) depends on its oceanic resolution¹⁸: as a consequence, higher resolution models are the most suited to simulate the precipitation over the Amazon region, also considering the typical small-scale variability of precipitation fields.

Hence, it is the purpose of this research to frame the projections of end-of-century Amazon rainforest in the set of its equilibrium states, making use of the outputs of a ultra high resolution coupled climate model and a coupled biogeography and biogeochemistry equilibrium biome model. The use of an ultra high resolution climate model will allow us to capture (ocean-related) precipitation variability with the highest accuracy possible. Employing a biome model for the rainforest will enable us to explore its spatially-resolved equilibrium states in a wide range of climatic parameters, understanding the dynamics of the rainforest under imposed climate change, and how future climate projections fit in the context of a wider set of equilibria.

Chapter 2 *Methods and Models* includes an explanation of the sources and methods used to simulate and assess the climate and biome types in the Amazon rainforest, both in the present and in the future. Chapter 3 *Amazon climate modelling* summarises the results of the validation of climate models and the esti-

mation of changes to the Amazon climate under climate change. Chapter 4 *Amazon vegetation modelling* investigates the response of the rainforest to different climatic anomalies, presents the projected biome distribution for end-of-century under climate change, and outlines a method to include a simple vegetation feedback in a biome model. Chapter 5 *Discussion and Conclusion* tries to summarise and comment our results, framing them in the context of past and possible future research.

2. Methods and Models

2.1 Numerical Simulation of the Amazon climate

Prior to any investigation on the Amazon rainforest, the present-day Amazon climate had to be assessed, via means of models and observations, and the extent of projected climate change had to be estimated.

2.1.1 Data

Three sets of data were used in this research: observational data, to validate the goodness of fit of numerical models at predicting the climate in the region; a fully-coupled climate model with realisations with different resolutions; a selection from the latest Coupled Model Intercomparison Project (CMIP6). The observations and model characteristics are summarised in table 2.1.

ERA5 reanalysis (observational) data (doi.org/10.24381/cds.adbb2d47) was used as a reference for the present-day precipitation in the region. Present-day time was taken as a 25-year interval from 1993 to 2017. ERA5 horizontal resolution is 0.25° , with hourly and monthly-averaged output.

The Community Earth System Model (CESM) is a fully-coupled global circulation model. Its version 1.0.4 (hereafter CESM1) was run by Utrecht University at an atmospheric resolution of 0.25° , 0.5° and 1° (from here on regarded as Ultra High Resolution *UH*, High Resolution *HR*, Low Resolution *LR* respectively). The ocean resolution are 1° for LR and 0.1° for both UH and HR. HR and LR have one single realisation, UH has five ensemble members. LR and HR are present-day control simulations. The UH simulations are branched off from a 0.5° atmosphere simulation where the atmospheric pCO₂ was increased by about 1% each year (model years 2000-2100). UH ensembles were initiated near the beginning (CESM1 UH PD, model years 2003-2007) and end (CESM1 UH FU,

model years 2093-2097) of such simulation. UH has 3-hourly sums for precipitation and monthly-averaged output, HR and LR only monthly. All the CESM1 versions have fixed vegetation, thus the model does not account for any vegetation feedback, nor deforestation.

A selection of nine models from the Coupled Model Intercomparison Project-6 (CMIP6) models was obtained from Earth System Grid Federation (ESGF) archives (<https://esgf-node.llnl.gov/search/cmip6>) for the historical period. Due to CMIP6 data structuring, present-day was taken as a 15-years interval from 2000 to 2014 in these models. The horizontal resolutions of the CMIP6 atmospheric models are different.

2.1.2 Evaluation of Present-day and Future Climate

As previously mentioned, precipitation, CO₂ concentration and deforestation are the three parameters considered to play an important role on the health of the Amazon rainforest. The role of CO₂ concentration in atmospheric (thermo-)dynamics is accounted for in the settings of the different climate models. Deforestation will not be accounted for due to its absence in the selected climate models and unpredictable development in the future.

To assess the goodness of different numerical climate models in simulating present-day precipitation in the Amazon basin, a latitudinal-longitudinal box was defined, roughly sharing its boundaries with the Amazon rainforest. The box has dimensions of 74W-55W, 12S-5N (see Figure 2.1.a). Literature does not have consistent definitions of the rainforest basin, and the strong local variations produce significant changes in precipitation box-averages according to the box definition.

The spatially-averaged monthly climatology of precipitation of each model was analysed and compared to ERA5. Each model output was interpolated onto the ERA5 grid. We determined the root mean square (RMS), sum over time, and standard deviation (STD) of the difference between ERA5 and each climate model.

The time-mean difference (spatial 2D data) of each model with ERA5 observations was taken, and the spatial variations were analysed, accounting for the peculiarities of the topography of South America (see Figure 2.1.a). In fact, the north-most part of the box (the region of Gran Sabana, in southeastern Venezuela, western Guyana) contains table-top mountains called Tepui, which prominence (up to 1000m) complicates the simulation of the atmospheric flows above and around them. Higher resolution models have the capability of better represent-

Table 2.1: Fully-coupled climate models used in this work with their spatial resolution.

No.	Origin	Model name	Atmospheric resolution	Ocean resolution	Temporal resolution	no. of members	Variant label	Time period
1	Utrecht University	CESM1 UH	0.25°	0.1°	3h, monthly	5	n.a.	2003-2007 (PD), 2093-2097 (FU)
2	Utrecht University	CESM1 HR	0.5°	0.1°	monthly	1	n.a.	2000-2025
3	Utrecht University	CESM1 LR	1°	1°	monthly	1	n.a.	25 years of control run
4	CMIP6	CESM2	2°	2.25°	monthly	1	r11p1f1	2000-2014
5	CMIP6	MCM	2.25°	2.25°	monthly	1	r11p1f2	2000-2014
6	CMIP6	MIROC	2.75°	1°	monthly	1	r11p1f2	2000-2014
7	CMIP6	INM	1.5°	1°	monthly	1	r51p1f1	2000-2014
8	CMIP6	BCC	1°	1°	monthly	1	r31p1f1	2000-2014
9	CMIP6	CMCC	1°	1°	monthly	1	r11p1f1	2000-2014
10	CMIP6	CNRM	0.5°	1°	monthly	1	r11p1f2	2000-2014
11	CMIP6	IPSL	1.25°	1°	monthly	1	r91p1f1	2000-2014
12	CMIP6	HadGEM	0.5°	0.25°	monthly	1	r11p1f3	2000-2014

ing the topography-induced atmospheric flow variations, whereas lower resolution models intrinsically smooth out high prominence mountain ranges.

CESM1 UH PD data were grouped in day-of-year, and the resulting climatology was compared with ERA5 hourly data. The Probability Density Functions of precipitation of CESM1 UH PD were compared to ERA5 ones.

Literature marks the importance of the dry season length for the health of the Amazon rainforest. However, there is no consensus over the definition of “dry season”: Sampaio et al.¹⁹ and Jackson et al.¹³ consider boreal meteorological summer (June-August) to be dry season; Yoon and Zeng⁶ consider June-October as dry season; Salazar and Nobre¹⁰ do not explicitly define “dry season”, even though they mention its lengthening. It was our objective to develop a method that avoided any arbitrarily chosen value and could be applied to regions with different climatological characteristics. A virtuous example is the work of Costa and Pires²⁰, who used a fixed threshold of 3.5 mm/day based on yearly-averaged evapotranspiration data. Although in principle this approach is independent on the region of interest, and lacks any arbitrariness, the definition (and consequent calculation) of evaporation and transpiration data varies between different models and observations: as a consequence, a meaningful comparison between data sources cannot be performed.

Hence, we developed a method to evaluate the dry season length which makes use only of precipitation data, does not have any arbitrary temporal or magnitude guesses, and allows to compare different datasets. Starting from the end of the wet season (when precipitation starts decreasing), and continuing until the lowest precipitation day, we calculate the time needed for precipitation to reach the same value again. We call this time “precipitation recovery lag” (indicated by τ). The result includes all the possible dry season durations with a fixed magnitude threshold, as well as gives information about the shape of the precipitation climatology during the dry season. An example is shown in Figure 2.1.

In order to evaluate the spatial and climatological changes of precipitation in the end of the century, CESM1 UH FU was compared to CESM1 UH PD using the same methods as in PD-ERA.

2.2 Biome model - BIOME4

As vegetation is fixed in the climate models we have used, it is not possible to analyse changes in biome type over time. Therefore, a biome model was used to investigate the response of the Amazon rainforest biomes to different climate

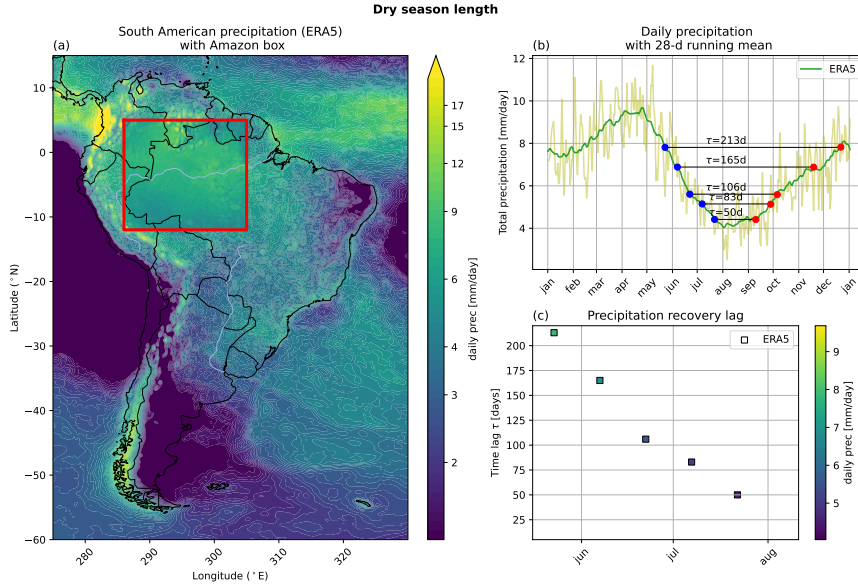


Figure 2.1: South American precipitation, with our Amazon box, together with an exemplification of our measure of the dry season length. Panel (a) shows our Amazon box (red square) superimposed on the precipitation field for South America as in ERA5 observations. The table-top mountains mentioned in the text (Tepuis) are located in the North of the box (they correspond with the local peaks of precipitation). Panel (b) shows the daily precipitation (light green) from ERA5 observations, with a superimposed 28-days running mean (dark green). The five blue dots indicate random (example) days between the maximum and the minimum of precipitation intensity (May-August), and the red dots the first day when precipitation reaches the same value. τ indicates the time lag in days (“Precipitation recovery lag”). Panel (c) shows the length of τ depending on the prescribed onset of the dry season (position of the blue dot). The colour indicates the strength of the precipitation connected to that τ (i.e. the ordinate of the horizontal line in panel (a)).

conditions.

BIOME4²¹ is a coupled biogeography and biogeochemistry equilibrium model which simulates the equilibrium distribution of 28 major potential biomes. It implicitly simulates competition between plants.

Table 2.2 summarises its inputs and table 2.3 summarises its outputs. Of all the outputs, only the biome type will be used in this research.

For each set of input data and parameters BIOME4 finds the biome type (plant functional type, *PFT*) that maximises the net primary productivity (NPP) in every gridcell. Thus, per gridcell there is only one possible biome type. Semi-empirical rules are used to discern whether woody PFTs or grasses will dominate in a gridcell. Being an equilibrium model, it cannot give information on multiple biomes being possible for the same set of climatic conditions, nor on temporal dynamics. BIOME4 has a spatial resolution of 0.5° and comes with an input dataset (hereafter called the *original* input).

Table 2.2: BIOME4 inputs description

<i>variable</i>	<i>unit</i>	<i>attributes</i>
precipitation	mm/mo	spatial, 12 months
temperature	d°C	spatial, 12 months
absolute minimum temperature	d°C	spatial, single value
percent of possible sunshine	%	spatial, single value
soil water holding capacity	mm/m	spatial, 2 vertical layers
soil water percolation index	mm/hr	spatial, 2 vertical layers
CO ₂ concentration	ppm	global average, single value

Table 2.3: BIOME4 outputs description

<i>variable</i>	<i>units</i>	<i>attributes</i>
Biome type	integer [1,28]	spatial, single value
Net Primary Productivity (NPP)	gC/m ²	spatial, single value
Decomposition scalar	integer	spatial, single value
Leaf Area Index (LAI)	gC/m ²	spatial, single value
Total annual runoff	cm	spatial, single value
Monthly runoff	cm	spatial, monthly
Coldest month	integer [1,12]	spatial, single value
Growind Degree Days (GDD)	integer	spatial, single value

To give support to runs of BIOME4 with the original input and with CESM1 UH inputs, we had to compare the original input with CESM1 UH. Of the inputs of table 2.2, only precipitation and temperature were analysed: absolute minimum temperature is assumed not to change under a warmer climate; sunshine percentage could be different under an altered water cycle and atmospheric dynamics, but the matter is out of our scope; soil characteristics could change with a changing biome, but it is out of the scope of this research to investigate that. Supplementary figures S1 and S2 show the comparison between original precipitation and temperature with CESM1 UH (PD and FU). The differences in intensity and spatial distribution are significant, hence we decided to scale both precipitation and temperature CESM1 UH fields according to

$$scaledField_{ensemble,year}^{period} = originalField \cdot \left(1 + \frac{CESM_{ensemble,year}^{period} - \overline{CESM}^{PD}}{\overline{CESM}^{PD}} \right) \quad (2.1)$$

\overline{CESM}^{PD} indicates the mean over the five ensemble members for present-day. The subscript *year* ranges from 1 to 5 and represents the 5 years of each ensemble member of CESM1 UH. *period* can either be "present", or "future". This method gives us 25 years for both present-day and future. By definition, the mean of the 25 years of the present-day data is equal to the original field.

3. Amazon climate modelling

3.1 Present day precipitation

Most of the models spatially underestimate the present-day precipitation in the region (see Figure 3.1.b). There are four model points (CESM1 UH, CESM1 HR, INM, HadGEM) which are closest to the origin, thus being the ones where the difference with ERA5 observations is either the smallest (low RMS) or least variable over time (low STD). Regardless of which L^p norm is used, the point representing CESM1 UH is the closest to the origin. Nevertheless, CESM1 UH still shows biases with respect to observations.

CESM1 UH PD mostly shows a spatial underestimation of precipitation in the box (Figure 3.2, panel (b)). An opposed bias is seen in the Northern region (where Tepuis are), where supposedly the model resolution does not resolve the peculiar prominence of the topography. The regionally-averaged underestimation is equally visible in the climatology (panel (a) of the same figure): from February to June CESM1 UH simulations overlap with ERA5 observations, whereas from July to January there is a 1-2 mm almost constant underestimation. The model's inability to properly simulate extreme events is evident (see the probability density function *PDF* on panel (c) of Figure 3.2). The marked positive skewness of the PDF of ERA5 ($\tilde{\mu}_3=1.15$) is not properly represented by the CESM1 UH ($\tilde{\mu}_3=0.26$). Nonetheless, opposed to the higher percentiles, the lower percentiles are well represented (<1 mm/day error), if not slightly overestimated. CESM1 UH PD consistently overestimates the length of the dry season (see Figure 3.2.d): with a maximum overestimation of about 70 days if the dry season is defined to start in June, it reduces until matching with observations when the dry season is defined to start in July.

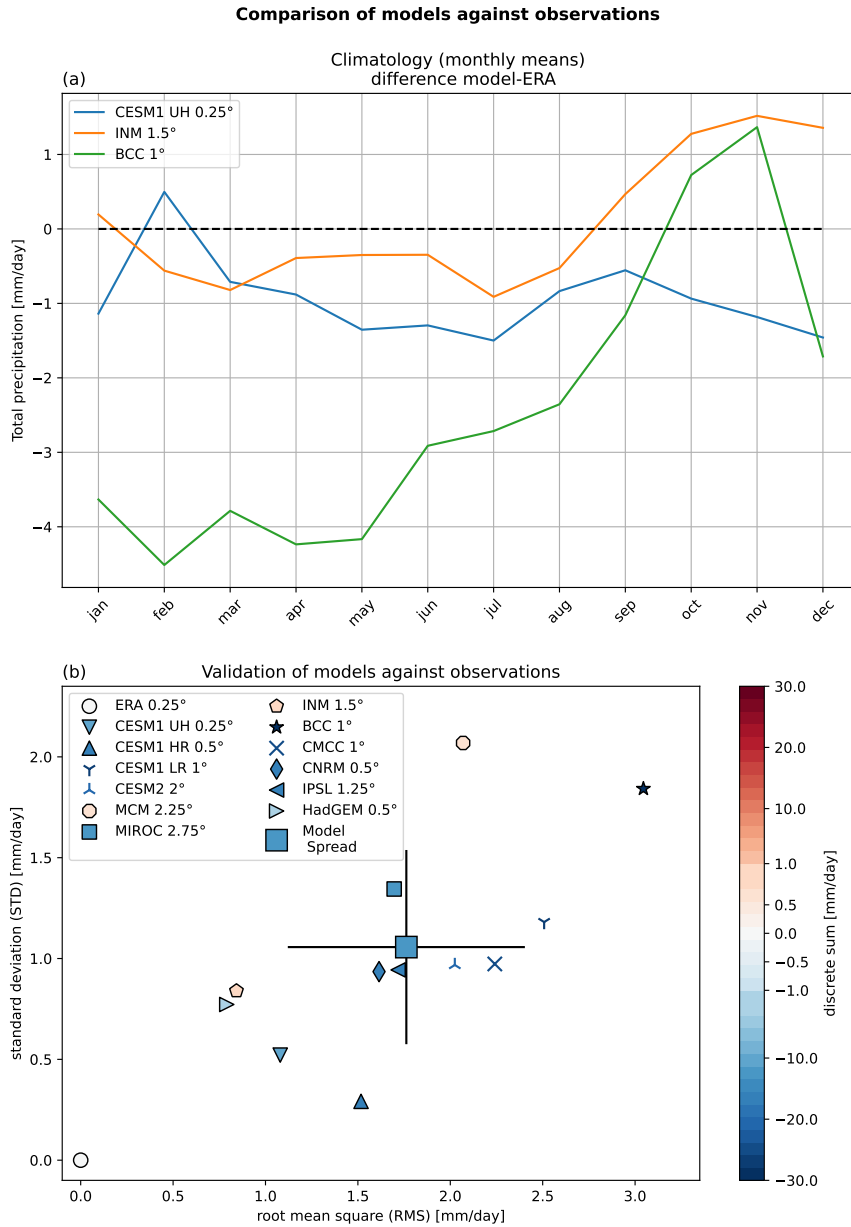


Figure 3.1: Validation of different models against observations. Panel (a): Difference of selected climate models with observations. Each model is represented by a solid line, the zero line (black dashed) indicated a “perfect” model, the one that coincides with observations. A model that constantly over-/underestimates is considered to perform better, as a homogeneous over-/underestimation indicates that the model is able to properly reproduce the monthly variability of precipitation, and the scaling defined by equation 2.1 can efficaciously counteract homogeneous biases. Panel (b): Each point corresponds to a climate model, and the big square dot indicates the model spread (the position of the point is the x, y average, the errorbars are the x, y standard deviations). We took the difference between model and observation, and calculated the root mean square RMS (x-axis) and standard deviation STD (y-axis). The colour of each point indicates the time integral (discrete sum) of such difference. Note that the colorbar is not homogeneous, but bilinear. Each legend entry includes the atmospheric spatial resolution of each model.

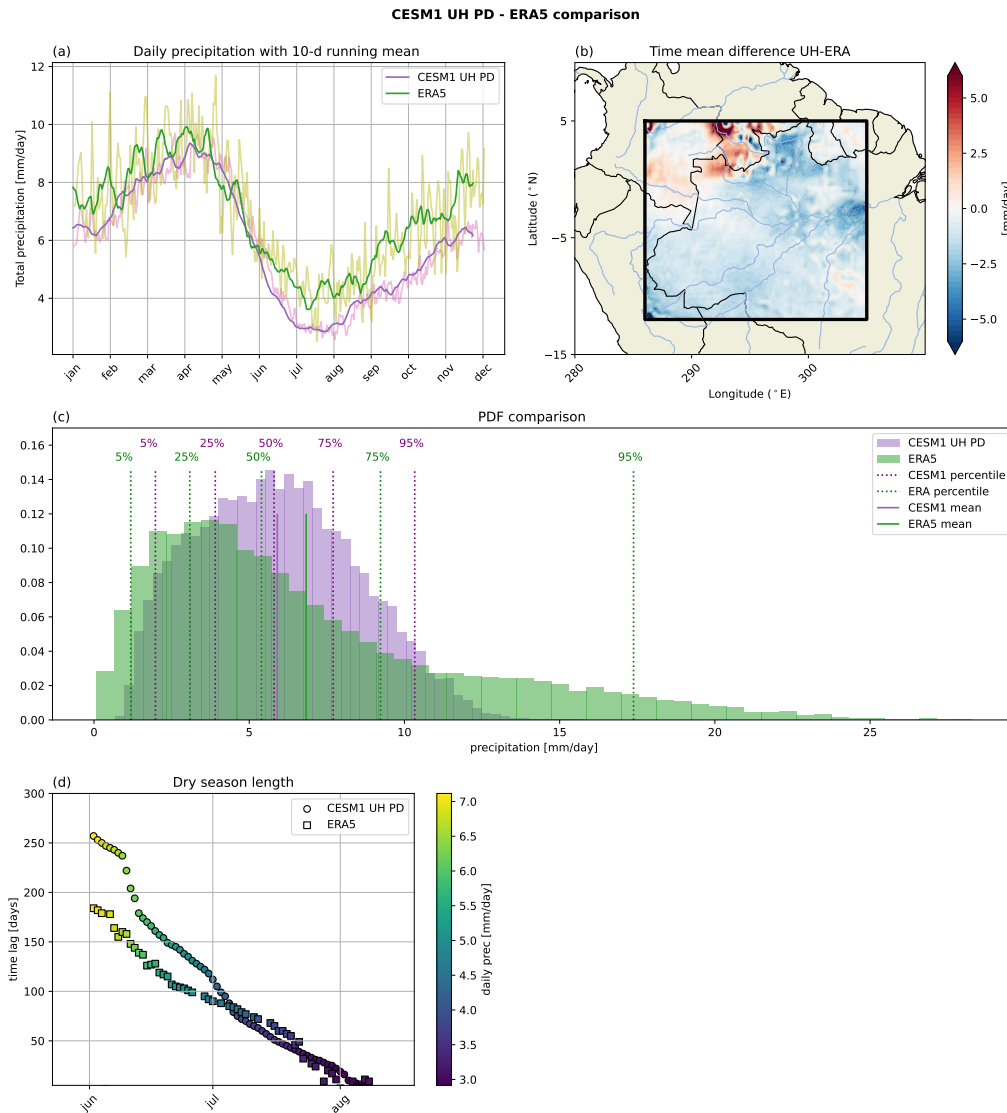


Figure 3.2: Comparison between ERA5 observations and CESM1 UH PD climate model. Panel (a) shows the daily precipitation (lighter colors) with a superimposed 10-days running mean (darker colors). Panel (b) shows the time mean differences between model and observations. Panel (c) includes the comparison of the two probability density functions PDF: the histograms are the distributions of precipitation (time and space averaged); the solid lines are the means (first moment); the dotted lines are different percentiles. Panel (d) compares the dry season length with the method explained in section 2.1.2 (see caption of fig. 2.1 for further clarification): round dots refer to CESM1 UH PD values; square dots refer to ERA5 values.

3.2 End-of-century precipitation

End-of-century simulations do not project a spatially homogeneous change: an increase of precipitation of 15% at most is projected in roughly the South Western half of the box; the North Eastern one sees a non-uniform similar-in-strength decrease, although local exceptions are present (Figure 3.3 panel (b)). Overall, the annual mean precipitation is expected to decrease from 5.90mm/mo to 5.31mm/mo (-10%). The distribution of precipitation is expected to uniformly shift towards lower values (same figure, panel (c)), but no significant change is projected in extreme events values or intensity (see the change in location of the high percentiles). The skewness $\tilde{\mu}_3$ is projected to change from 0.26 of the PD data to 0.46 of FU.

As for the climatology, the data projects a consistent lengthening of the dry season. Depending on the definition of the start of the dry season, the lengthening ranges from around 10 days to over 50 days. With a dry season that starts in June, the lengthening is about 1 month.

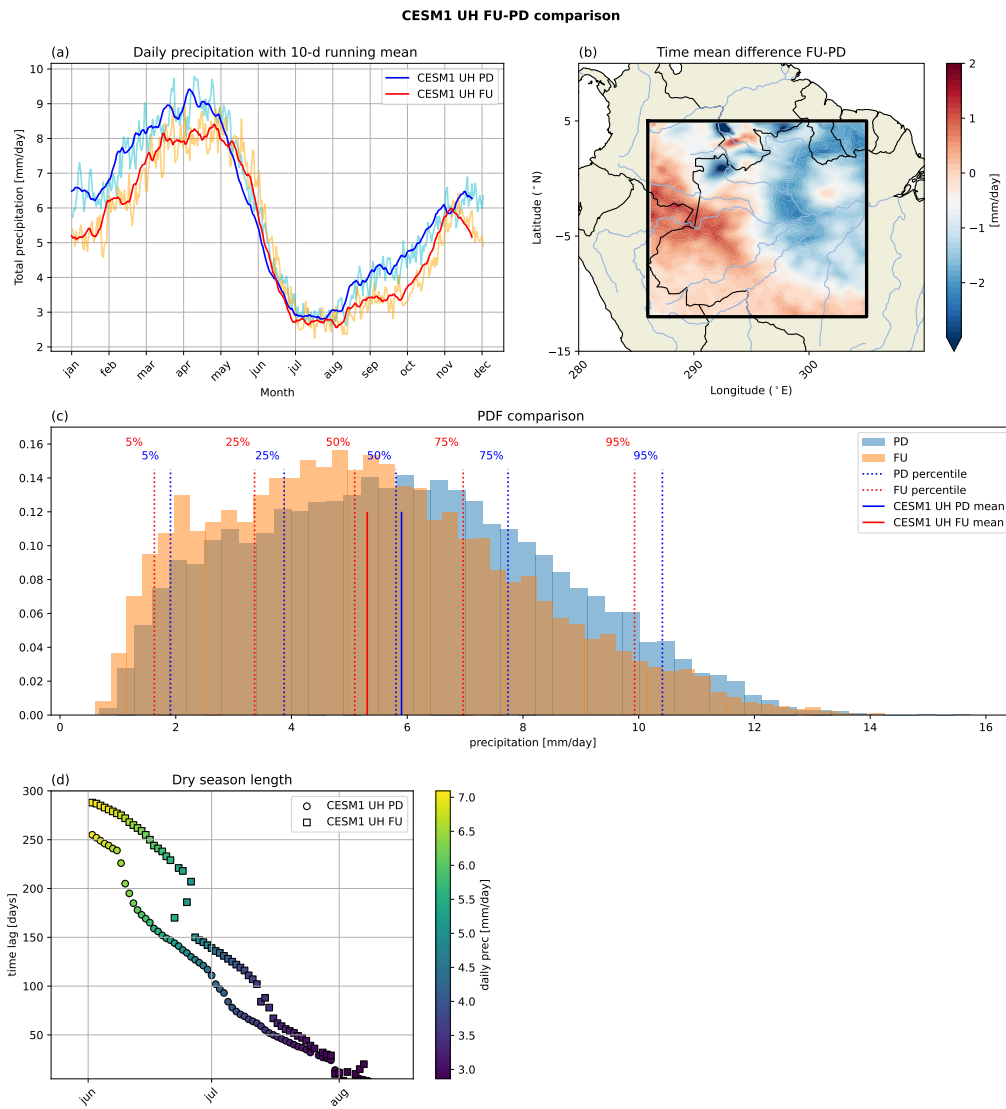


Figure 3.3: Similar to figure 3.2 but the comparison is between CESM1 UH PD and CESM1 UH FU

4. Amazon vegetation modelling

The Amazon rainforest was masked with the data from van der Laan et al.²² (see the red contour of Figure 4.5), bilinearly upscaled to match the output resolution of BIOME4 (0.5°). In sensitivity analyses, cover fractions of each biome were calculated over the masked region. Biome types were divided in two categories: *combined trees*, including tropical evergreen forest, tropical deciduous forest, tropical semideciduous forest, tropical conifer forest; *combined dry biomes*, including savanna and xerophytic shrubland (see the legend of Figure 4.5 for the full list of simulated biomes).

4.1 Sensitivity to absolute warming/drying

The response of the Amazon rainforest to a spatially and temporally uniform change in temperature and precipitation was investigated. Although literature suggests that temperature is not a dominant driver for changes in the Amazon rainforest, the spatial and magnitude differences for the temperature input shown in Figure S2 brought us to include temperature in this analysis. For every couple (temperature, precipitation), a run was performed. The annual average temperature over the mask ranges from 24°C to 39.5°C; the annual average precipitation over the mask ranges from 210 mm/mo to 70 mm/mo. Note that the prescribed variations exceed in magnitude any reasonable variations due to anthropogenic climate change. An idealised depiction of the applied changes is shown in Figure 4.1 panel (a). CESM1 UH PD and FU points were included in the results with the method explained by equation 2.1.

The response of the Amazon rainforest is dominated by precipitation changes (see Figure 4.2). Except for low variations (for an average temperature change of -1°C~+2°C), where a temperature increase induces an increase of trees at the expense of dry biomes, the rainforest response is almost independent of tem-

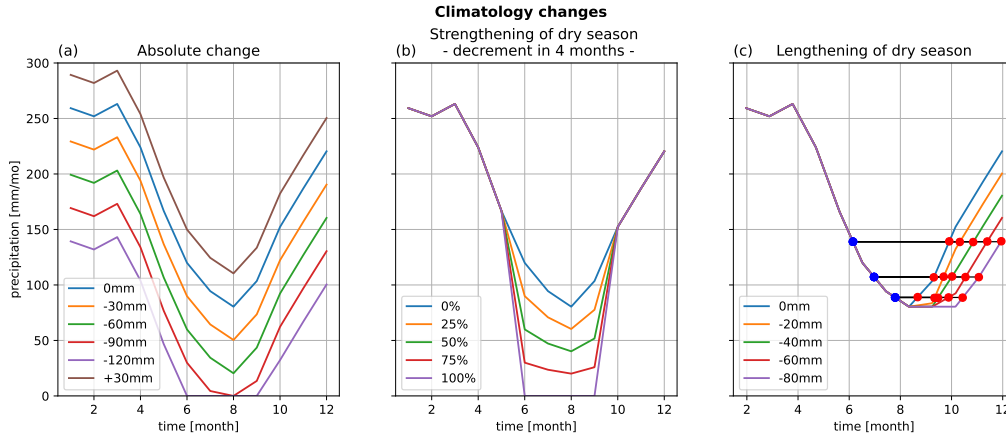


Figure 4.1: Exemplification of the changes to the climatology used in sensitivity analyses. Panel (a) shows a simplified version of the changes applied in the work of section 4.1: a spatially-uniform alteration of precipitation and temperature (the latter not shown in the figure) was applied to the climatology; each line corresponds to an alteration with a different intensity; if the values were to become negative, they were substituted with zero (see “-120mm” line). Panel (b) shows the strengthening of the dry season applied to the driest four months (see section 4.3): at each step (5 in the figure) a decrease of X% is applied to the driest months, until the precipitation is zero for those months. Panel (c) shows an exemplified version of the lengthening applied in section 4.2: from the driest month until the end of the year, precipitation has been uniformly reduced; in the months where the values become lower than the original driest month, precipitation has been set to the original driest value; the blue and red dots are to indicate the beginning and end of the dry season (as defined in section 2.1.2).

perature. On the contrary, a decrease of precipitation of about 15 mm/month generates a reduction of 10% of trees, replaced by dry biomes. This response is widely homogeneous throughout the investigated range of precipitation decrease. Future projections indicate a reduction of around 15% in the tree cover, and a simultaneous increase of a similar percentage in dry biomes. Future and present-day precipitation yearly averages are incompatible under the assumption of the distributions being Gaussian (z -test result $\sim 10^{-11}$). Note that this sensitivity analysis only considers averages of temperature and precipitation over the mask. Then, it is possible that an analysis that accounts for the spatial variations could produce different future projections (see Section 4.5).

4.2 Sensitivity to lengthening of the dry season

We have investigated the response of the Amazon rainforest to a lengthening of the dry season, consistently with what expressed in section 2.1.2. We uniformly decreased precipitation in the months from the driest until the end of the year: this way, we have effectively lengthened the dry season according to the definition

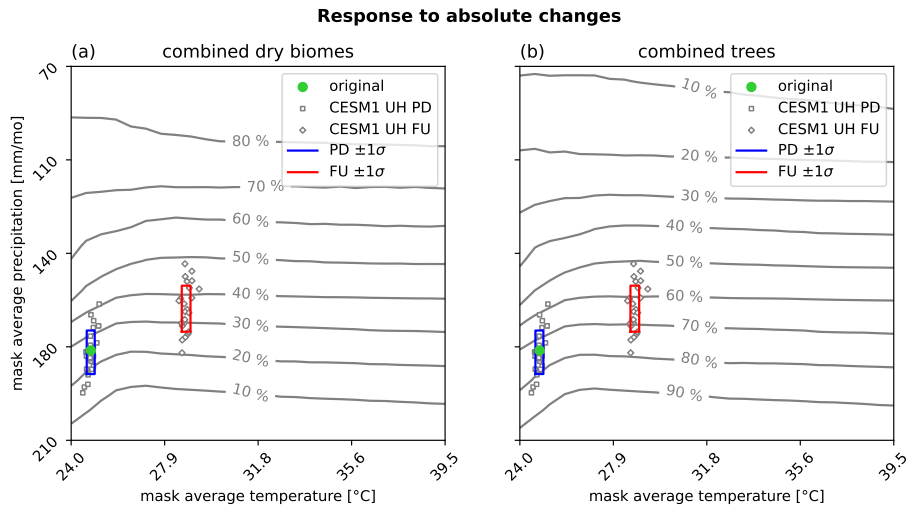


Figure 4.2: Simulated response of the Amazon rainforest to spatially uniform changes of temperature and precipitation. The simulated fraction over the Amazon rainforest of dry biomes (*savanna* and *tropical xerophytic shrubland*, panel (a)) and trees (*tropical evergreen forest*, *tropical deciduous forest*, *tropical semideciduous forest* and *tropical conifer forest*, panel (b)) are plotted as contour lines. The original input values are plotted in both panels as a green dot (it corresponds to “zero changes” for precipitation and temperature). Scaled yearly inputs from CESM1 UH are plotted as square dots (present-day) and round dots (future) in both panels. Panels also include an estimation of the spread of PD and FU points: the blue and red squares are delimited by ± 1 standard deviation in both coordinates. Statistically (under the assumption of independent coordinates), 46.5% of the points fall inside the squares.

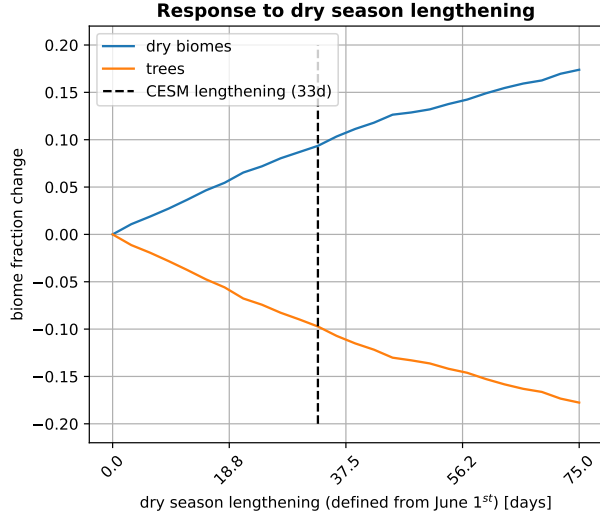


Figure 4.3: Simulated response of the Amazon rainforest to a lengthening of the dry season (as defined in section 4.2, and exemplified in panel (c) of figure 4.1). Precipitation was decreased after it had reached its minimum value, producing a lengthening of the dry season. Note that our measure of the length of the dry season depends on where it is defined to start: for plotting purposes it is defined to start on June 1st (other choices would scale the x-axis). The simulated fraction over the Amazon rainforest of dry biomes (*savanna* and *tropical xerophytic shrubland*) and trees (*tropical evergreen forest*, *tropical deciduous forest*, *tropical semideciduous forest* and *tropical conifer forest*) are plotted. The black vertical dashed line is the projected lengthening of the dry season from CESM1 UH when it is defined to start on the 1st of June.

of section 2.1.2. Panel (c) of figure 4.1 shows an exemplified version of the applied lengthenings. The response of the rainforest is linear for the whole range of investigated lengthenings (see Figure 4.3), and dry biomes substitute trees as the dry season is lengthened. When the dry season is lengthened by 75 days, the projected biome shift is about 17%. Note that a >2.5 months lengthening is unlikely even under the worst climate change scenarios. The relative lengthening of the dry season in the future CESM1 UH compared to present-day generates a 10% increase of dry biomes, at the expense of trees.

4.3 Sensitivity to strengthening of dry season

Hereafter we propose a sensitivity analysis to an increasing drying of the n driest months. For each run, the precipitation of the driest n months (with $n \in [1, 5]$) was decreased until it reached zero. Note that zero average precipitation in the driest months is unlikely even under the worst climate change scenarios. Temperature was not altered in this analysis. Panel (b) of figure 4.1 shows a exemplified climatology alteration. As for CESM1 UH, we determined the change in average precipitation in the n driest months.

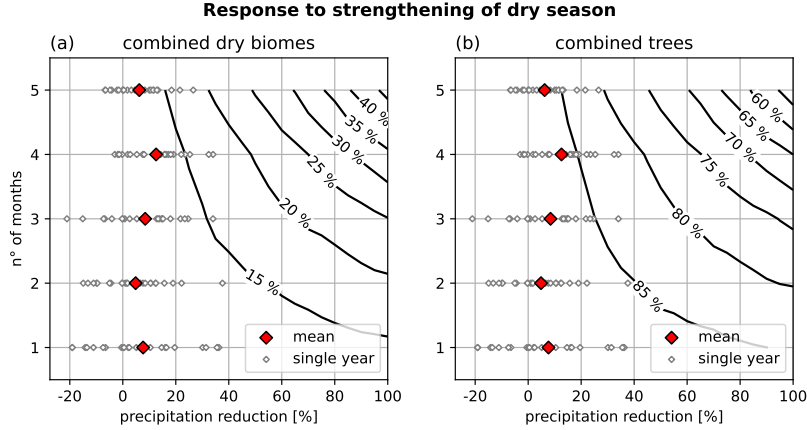


Figure 4.4: Simulated response of the Amazon rainforest to a strengthening of the dry season (as defined in section 4.3, and exemplified in panel (b) of figure 4.1). Precipitation was reduced in the n driest months (y-axis) in percentage steps (x-axis). The simulated fraction over the Amazon rainforest of dry biomes (*savanna* and *tropical xerophytic shrubland*, panel (a)) and trees (*tropical evergreen forest*, *tropical deciduous forest*, *tropical semideciduous forest* and *tropical conifer forest*, panel (b)) are plotted as contour lines. White diamonds indicate the mean precipitation variation on the n driest months of each future year compared to present-day mean (from CESM1 UH). Red diamonds are the means of all the white ones.

The resilience of the rainforest to short droughts is expressed by the relative independence of the biome fractions to precipitation reductions in the 1,2,3 driest months (see Figure 4.4). In fact, with a complete drying of the driest three months, the trees fraction only decreases of 10-15% (and the dry biomes fraction increases accordingly). When the reduction is applied to four and five months, dry biomes substitute trees for up to 35% of the masked area. The future projections' driest months are on average drier than their present counterpart (with numerous single-year outliers), but the average precipitation reduction never exceeds 20%. As a consequence, the dry-season-strengthening-induced biome changes does not exceed 5%.

4.4 Sensitivity to CO₂

To investigate the sensitivity of the Amazon rainforest to global CO₂ changes, we linearly increased the CO₂ concentration of the input from 413ppm (circa present day value) to 1200ppm (CESM1 UH FU value is 936ppm), and run BIOME4 at each step. Biome fractions on the masked region were calculated at each step. No significant change of the biomes fraction is present until values of pCO₂ of around 1050ppm, beyond the 2100 climate change value (see Figure S5).

4.5 BIOME4 with scaled input

The scaling method described by equation 2.1 allowed us to run BIOME4 with CESM1 UH FU data, to investigate the projected spatial changes of biome distribution over the Amazon rainforest. This analysis intrinsically includes (spatial) variations of all the parameters that are projected to change under climate change. As such, it is the closest available estimate of the end-of-century state of the Amazon rainforest under the prescribed climate change that BIOME4 can give.

Figure 4.5 reports the spatial distribution of biomes for the original input of BIOME4 and for an average of the scaled future projections. Spatially, the presence of a “core” of the Amazon rainforest is evident, where *tropical evergreen forest* dominates, centered around 0°N, 285°E, which is not projected to change substantially under climate change in the end of the century. On the other hand, major changes are visible South, South East and East of such core. *Savanna* and *tropical xerophytic shrubland* are projected to become dominant in large areas, at the expense of *tropical (semi-)deciduous forest*. In the mask, a decrease of tree fraction of 24% is projected, together with a simultaneous increase of the same percentage of dry biomes.

4.6 Evaporation advection scheme

In its setup, BIOME4 does not include any advection mechanism, and no feedback of vegetation on the atmospheric water content. We have attempted to include a simple evaporation advection scheme, which allows a feedback from vegetation to precipitation. Hereafter a brief outline of our method:

- Run BIOME4 with its original input.
- Separate BIOME4 output in dry biomes and trees (as done in previous analyses). Assign a fixed evaporation rate for the trees (E_f) and for dry biomes (E_d).
- Assume that a fraction p of the evaporated water remains in the gridcell, while the remaining is advected to the neighbouring cells.
- Include the vegetation-induced changes to the precipitation field and run BIOME4 again.

We have separated the precipitation field in a vegetation/time independent “large scale” field (LS) and a vegetation/time dependent “evaporation-precipitation”

	<i>North</i>		
	20%	5%	
<i>West</i>	50%	C	<i>East</i>
	20%	5%	
	<i>South</i>		

Table 4.1: Transport matrix of advected moisture from cell C to neighbouring cells. The percentages in the cells indicate how much of the water available for advection from cell C is advected to that cell.

(EP) field. LS has been calculated as the original precipitation input minus the initial vegetation feedback. Then, at every time, precipitation is defined as

$$PREC(t) = EP(t) + LS \quad (4.1)$$

Considering that the ERA5 evaporation yearly average for our Amazon box is 3.5mm/day, we assumed a E_f of 100mm/mo. E_d has been set to 50mm/mo. Evaporated water is advected westward, mostly zonally, according to matrix 4.6. The parameter p regulates the advection: with a value of p equal to 1, no advection takes place. A simplified - explanatory - description of the advection method is described in figure 4.6.

The efficacy of our method is proven by the westward transition to different biomes seen while integrating with a p parameter smaller than 1 (see Figures S7 and S6). Indeed, with p smaller than one, the forest reaches an equilibrium with fewer tree cover compared to the original output (see Figure 4.7.a). The number of timesteps necessary to reach equilibrium increases with decreasing p . Moreover, with a smaller p the amount of water leaving each cell is higher, and the forest sees a larger fraction of tree-covered gridcells that shifts to dry biomes. The response of equilibrium states of the rainforest to the p parameter is approximately linear (see Figure 4.7.b).

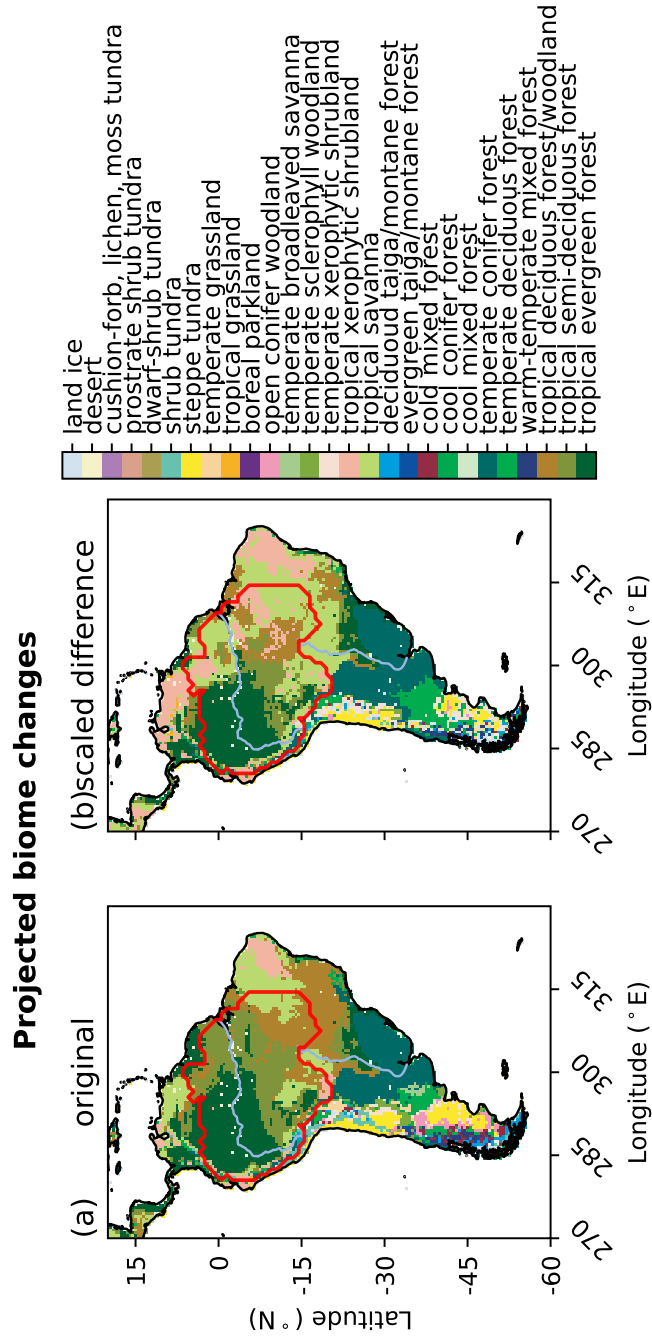


Figure 4.5: Simulated biome distribution for South America (with Amazon rainforest highlighted) in present-day and future. In both panels: the red contour is the mask of the Amazon rainforest from van der Laan et al.²²; the colours correspond to the biomes as in the legend. Panel (a) shows the result of running BIOME4 with its original input data. Panel (b) shows the result of a run with the scaled difference between CESM1 UH FU and PD, with the method explained in equation 2.1, scaling the mean of all future years with the present-day mean.

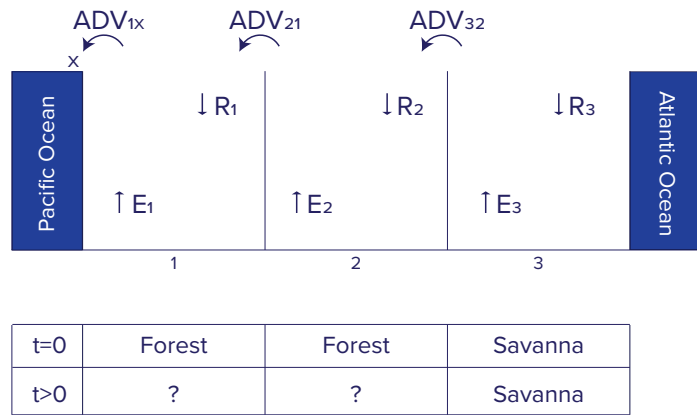


Figure 4.6: Schematic representation of the implemented evaporation advection scheme. In the example, the Amazon rainforest is zonally divided in three cells. Each cell has an evaporation E_i that depends on the biome present. In each cell, precipitation equals $R_i = pE_i$, with $p < 1$. Each cell advects $ADV_{ij} = (1 - p)E_i$ to its west-neighbouring j cell. Suppose that in the initial state ($t = 0$) the three cells are as the first row of the table. At $t > 0$ cells 1 and 2 could change state due to loss of water through advection. Note that cell 1 advects out of the boundaries, thus this method does not conserve total water.

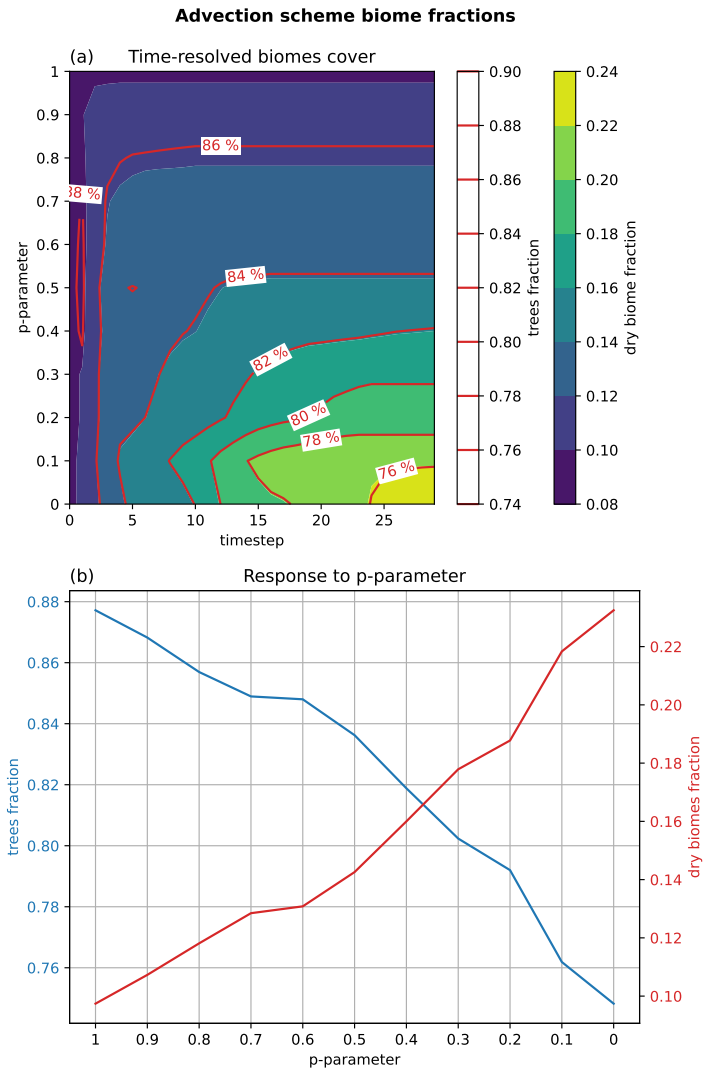


Figure 4.7: Results of the implementation of the evaporation advection method. Starting from the original output, the advection method was implemented across time. Panel (a) shows the biome fractions of trees and dry biomes for different values of the p parameter (y -axis), in time (x -axis). Panel (b) presents a cross-section of panel (a) at the last timestep. Thus, here the blue (trees) and red (dry biomes) lines indicate the equilibrium fractions for different p values.

5. Discussion and Conclusion

The present-day and end-of-century climate on the Amazon rainforest has been investigated by means of a fully-coupled fixed-vegetation high-resolution climate model (CESM1). Present-day simulations have been compared with a set of CMIP6 models, and against ERA5 reanalysis observational data. Future simulations have been run under 1% yearly pCO₂ increase. High-resolution CESM1 is among the fittest models to simulate the Amazon climate. The main inaccuracies lie in an overestimation of the length of the dry season and an underestimation of the skewness of the probability density function of precipitation. A 1-month lengthening of the dry season is projected for the future, together with an increase of precipitation intensity in the South West half of the region, and a decrease in North East half. Overall, the annual mean precipitation over the Amazon is projected to decrease of about 10%.

The comparison that we have performed between our CESM1 data, a selection of CMIP6 models and ERA5 reanalysis observations, reveals a diffused underestimation of Amazon precipitation throughout the state-of-the-art climate models. Future research should consider that this bias might result in an overestimation of dry biomes in the region.

An equilibrium biome model (BIOME4) has been used to investigate the sensitivity of the rainforest to different forms of climatic changes. The decrease of trees (and consequent, same-magnitude increase of dry biomes) deriving from a uniform reduction of precipitation in the region is simulated to be linear for a wide range of average precipitation anomalies. Projections for the future times fit well-within the linear response region. Temperature uniform changes play a minor role. A lengthening of the dry season is simulated to produce a decrease of trees (and an increase of dry biomes) which is linear with the magnitude of the lengthening. Climate change lengthening of the dry season is projected to induce a $\sim 10\%$ shift from trees to dry biomes. The strengthening of the dry season is expected to become important ($\gtrsim 15\%$ change) only when affecting at least four

months. The future dry season strengthening (compared to present day) is not projected to alter the biome distribution significantly. CO_2 has a second-order effect on the rainforest, compared to other investigated forms of climate change.

When BIOME4 has been run with the scaled output of future CESM1 results (thus simultaneously accounting for all the simulated forms of climate change), it projects a reduction of 24% of trees on the region and a increase of the same percentage of dry biomes.

Overall, these results produce a two-fold set of conclusions: on the one hand, a substantial shift of the Amazon rainforest to drier biomes is projected for the end-of-century under climate change conditions; on the other hand, the response of the rainforest is simulated to be linearly proportional to climate variations for a wide set of changes, with future projected changes laying well within the boundaries of the linear response region. The lack of non-linearities (and their consequences, such as abrupt changes or multiple equilibria) is probably due to the absence of vegetation feedbacks on the atmospheric circulation above the rainforest itself. Multiple studies^{5;23} highlighted how a significant part of Amazon precipitation originates within the rainforest itself, of which the majority has been transpired from vegetation. As dry biomes evaporate less water compared to trees, Amazon precipitation is expected to decrease as a consequence of shifts from trees to dry biomes. This could trigger a non-linear response where a precipitation decrease from climate change is magnified by the induced vegetation shift. To investigate whether non-linearities could be explored with BIOME4, we tried to account for the role of vegetation in the atmospheric water transport.

Our implementation of a simple vegetation feedback within BIOME4 has been successful in that the simulated rainforest has responded to advection of evaporation, which occasionally provoked biome shifts, which again changed the intensity of evaporation. However, multiple assumption and approximations lie behind our scheme. First and foremost, extracting a time/vegetation-independent large scale field from the total precipitation hides the assumption that the feedback of vegetation on global or continental atmospheric circulation is of a higher order compared to the feedback on the local. Furthermore, the description of the atmospheric flow in the rainforest has been over-simplified in our transport matrix: as reported by Boers et al.⁵, the atmospheric flow above the Amazon region rotates counterclockwise from westward close to the Atlantic ocean, to southwards towards the southmost edge of the region. Moreover, values of evaporation for trees (E_f) and dry biomes (E_d) have been “informedly guessed” based on other works^{20;5}, but not properly tuned. In fact, we reckon that analyses over the sensitivity of the model to different values of the parameter are necessary before drawing any physically meaningful conclusion from it. Similarly, we have not

investigated whether the p -dependent equilibrium that the rainforest reached was a mathematical equilibrium for the system, or a hiatus in the decrease of trees: as our model loses water at the western boundary (which is not recovered), we cannot exclude the constant decrease of available water will bring the rainforest to a different equilibrium, for a time sufficiently large.

Nonetheless, the relative success of our evaporation advection scheme in BIOME4 paves the way to more complex vegetation feedback implementations. BIOME4 accounts for soil characteristics, which are commonly either neglected²³ or simplified⁵, but it does not include any dynamics. Our work shows that BIOME4 does respond to vegetation-precipitation feedbacks. The response is towards decreasing trees, and increasing dry biomes: this suggests that including this feedback on end-of-century, climate-change projections would probably change the state of the rainforest even more (albeit limitedly). Note that our scheme could react to deforestation or forest fires: evaporation is altered after a biome shift regardless of the driver that generated it. Lastly, the method that we implemented allows for non-linear behaviours (which, at least mathematically, permit the existence of multiple equilibria and transitions between them): if the tree-covered equilibrium state of a cell was sustained by the advected water from the neighbouring cells, a shift of (one of) these could reduce precipitation enough for the cell to shift as well.

Concluding, in order to obtain the most valuable information over the Amazon rainforest, one should run a fully-coupled climate model with dynamic vegetation under an extensive set of climatic forcing, exploring both the spatial variations and possible multiple equilibria. However, with the current computational capabilities, this is too expensive. Similarly, the oversimplification of conceptual models limits the physical inferences drawable from their results. But, our vegetation feedback scheme efficiently realises a vegetation-atmosphere coupling, and could be extended to account for more complex atmospheric flows, which could be taken from the outputs of a high-resolution climate model, and the biome response could be investigated without running a fully-coupled climate model at every timestep.

Acknowledgements

The number of people that deserve a spot in this few paragraphs exceeds the limits imposed by the role of this section itself. Hence, I will shorten the list by explicitly thanking my supervisors, the Ocean and Climate group of IMAU, and my family and friends, with the hope that the others will still appreciate other forms of acknowledgement, rather than being mentioned hereafter.

My most sincere thanks is for Dr. René van Westen, for the contributions and support that he has given throughout the long process that this research has been. His cheerfulness, enthusiasm and sympathy risked overshadowing his knowledge and professional experience. He has been not only clear and detailed in his explanations, but he really cared for the success of this thesis and has always managed to find room to answer my doubts and correct my inaccuracies. Dr. Anna von der Heydt has guided the research with confidence and foresight, and has been a source of expertise and fruitful confrontation during the interpretation of the results. She never lost the big picture, and managed to re-orient the work when it was becoming too erratic. Prof. Henk Dijkstra's comments hit at the essence of this research, and contributed to fill gaps that would have become unforgivable mistakes.

Secondly, I value the inputs that came from the Werkbesprekings of the Oceans and Climate group. There, the environment sparkles with ideas and research is shared at every point. Multiple additions to this very work are traceable to questions or comments that came from members of the research group.

Lastly, I do not think I can exhaustively thank my family and my closer friends for all the support that they showed me whenever I needed some. Each in different way - on the phone from all over Europe, or during coffee breaks at IMAU, or even at home-, everyone has confirmed the reasons why I value their presence in my life.

Supplementary Figures

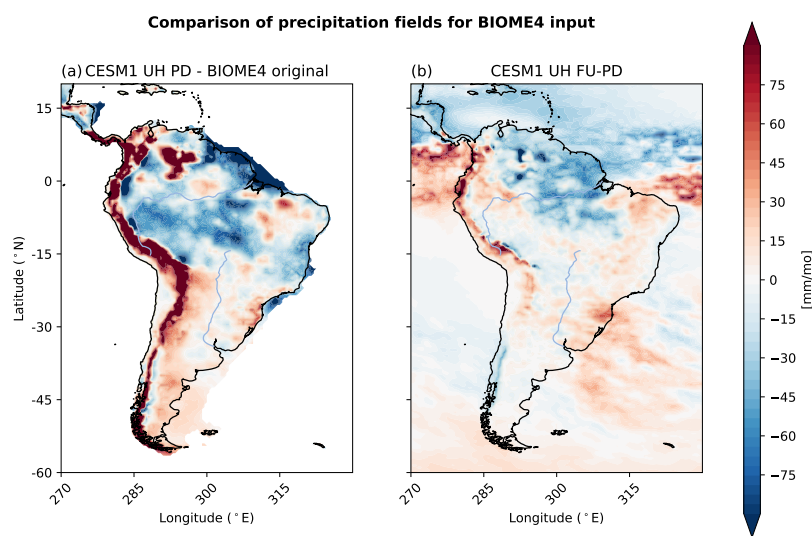


Figure S1: Comparison between different precipitation fields to be possibly used as BIOME4 input. Panel (a) shows the time-mean difference between the original BIOME4 input data and CESM1 UH PD. Panel (b) shows the time-mean difference between future and present-day for CESM1 UH results. Note that the original input only covers the land, while CESM1 UH has data also for the oceans: this will not affect the results because BIOME4 does not simulate atmospheric circulation, and in any case other spatial inputs are defined only on land (such as soil characteristics).

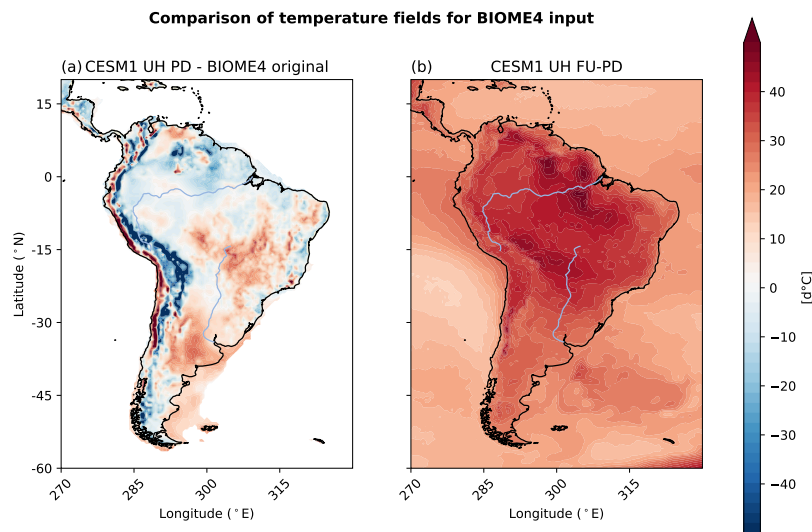


Figure S2: Comparison between different temperature fields to be possibly used as BIOME4 input. Panel (a) shows the time-mean difference between the original BIOME4 input data and CESM1 UH PD. Panel (b) shows the time-mean difference between future and present-day for CESM1 UH results. Note that the original input only covers the land, while CESM1 UH has data also for the oceans: this will not affect the results because BIOME4 does not simulate atmospheric circulation, and in any case other spatial inputs are defined only on land (such as soil characteristics).

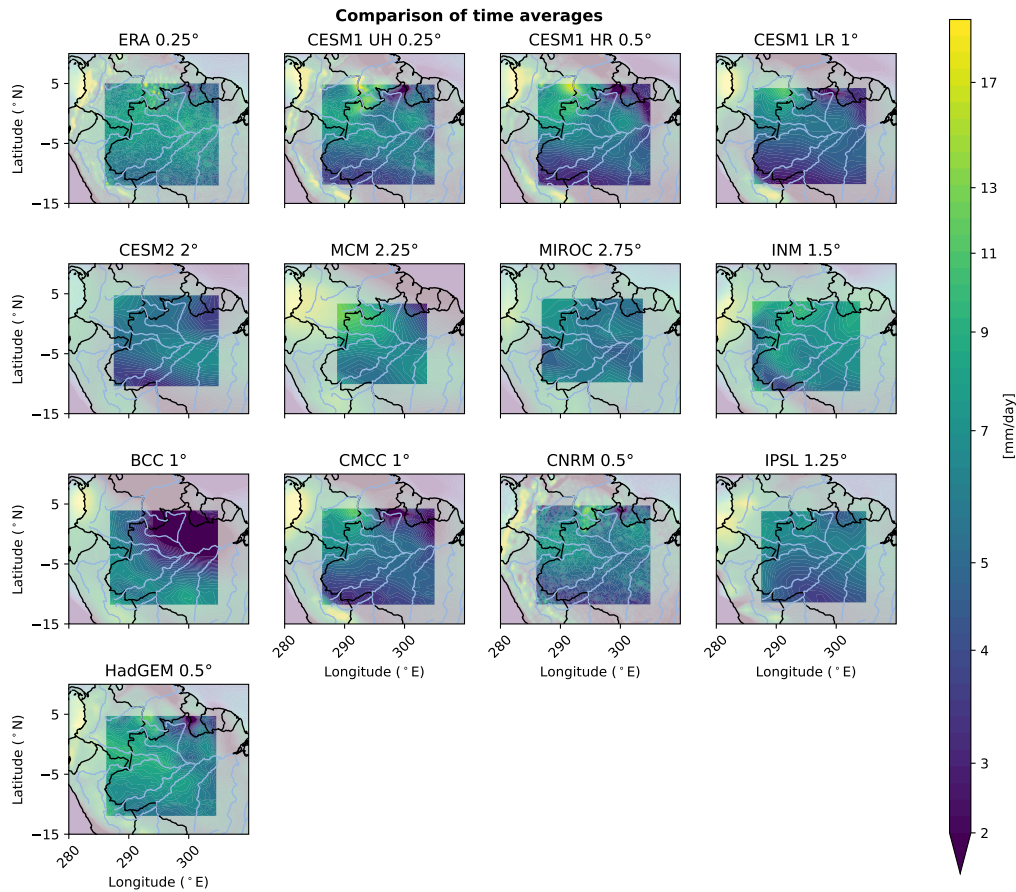


Figure S3: Time averages comparison between the precipitation for present-day from all the data sources used in this work. Each panel shows the time average of one model. Each title includes the spatial resolution of the model. The non-transparent area is the one corresponding to the Amazon box (see section 2.1.2), the semi-transparent area is shown for completeness. Note that the different spatial resolution produce a different size of the non-transparent area.

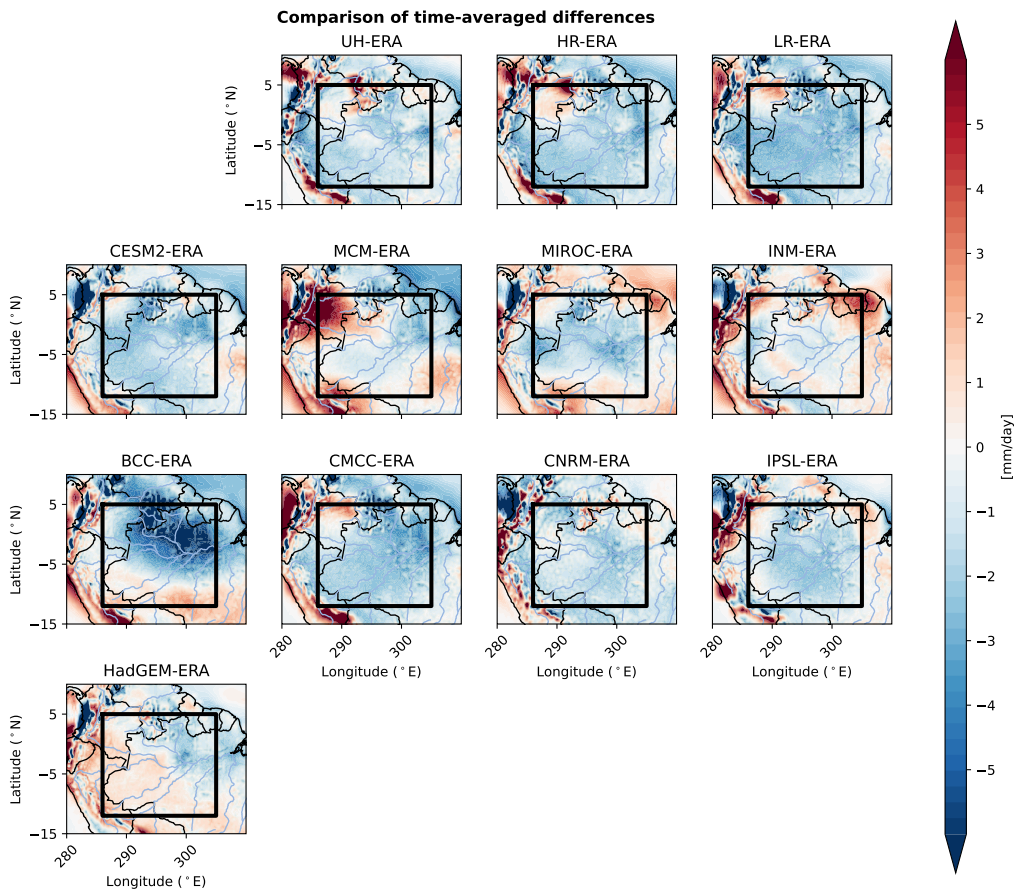


Figure S4: Time averages comparison between the precipitation differences between all the climate models used in this work and ERA5 observations. Each panel shows the time-mean difference of one model. The solid black contour corresponds to the Amazon box (see section 2.1.2). Note that all the models are bilinearly up-/down-scaled to match ERA5 observations.

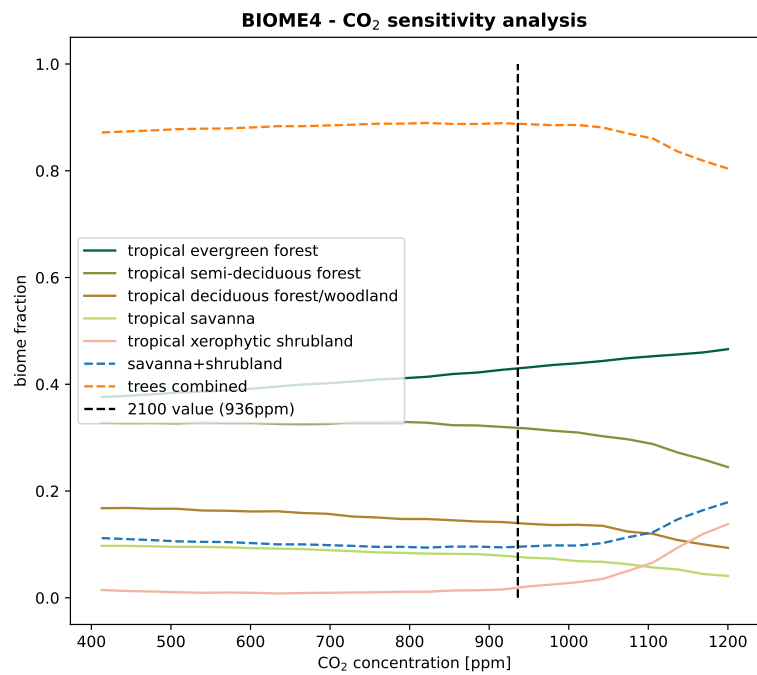


Figure S5: Simulated response of the Amazon rainforest to a change in CO₂ concentration. CO₂ concentration (x-axis) was increased in steps, and BIOME4 was run at each step. The simulated fraction over the Amazon rainforest of dry biomes (*savanna* and *tropical xerophytic shrubland*) and trees (*tropical evergreen forest*, *tropical deciduous forest*, *tropical semideciduous forest* and *tropical conifer forest*) are plotted, both separately and grouped. The vertical black dashed line is the CESM1 UH FU value.

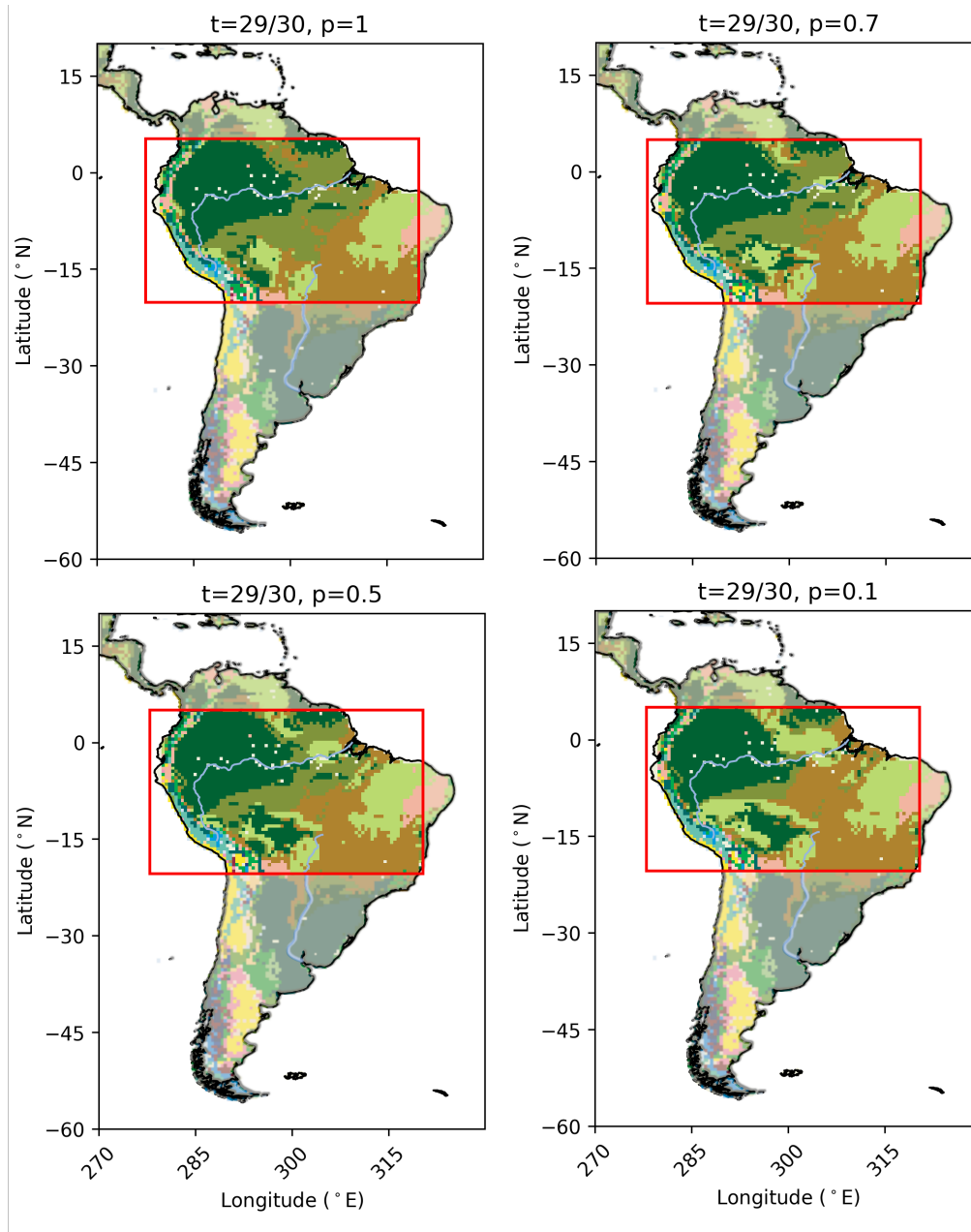


Figure S6: Dependency of the equilibrium states for the rainforest simulated with BIOME4 and our evaporation advection scheme on the value of the p parameter. The p parameter is indicated in the title of each panel, together with the timestep of each screenshot (all the integrations had already reached equilibrium). Colors correspond to biomes (see legend of figure 4.5). The evaporation advection method has been applied only inside the red box, the values outside are the ones of the original input of BIOME4. The results for $p = 1$ coincide with the original ones, as in that case no advection takes place. For decreasing p , the amount of water that is advected out of a gricell increases, and more cells shift to dry biomes.

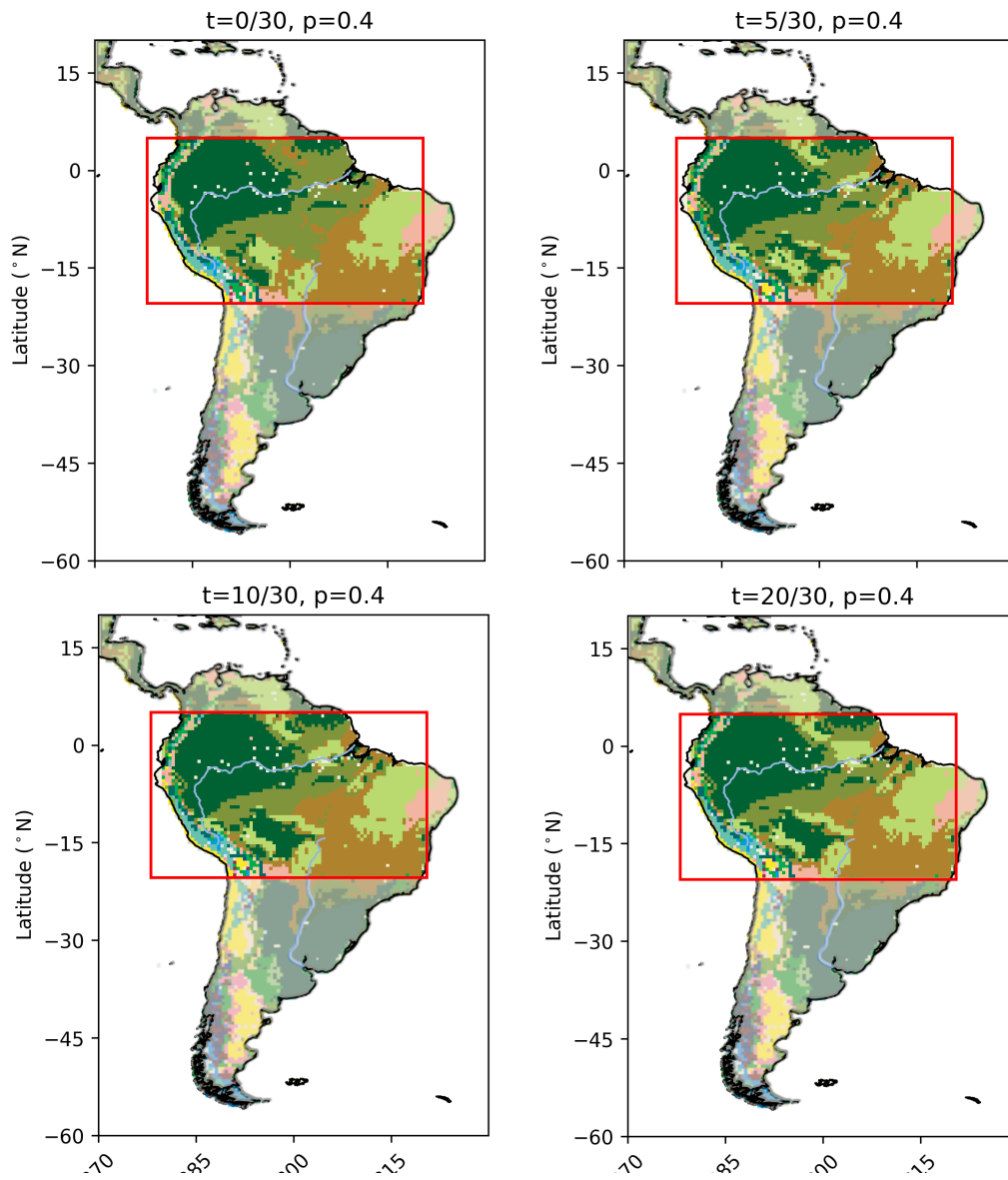


Figure S7: Variation of the state of the rainforest in time, as simulated with BIOME4 and our evaporation advection scheme, with a fixed p parameter. Colors correspond to biomes (see legend of figure 4.5). The evaporation advection method has been applied only inside the red box, the values outside are the ones of the original input of BIOME4. The results for $t = 0$ coincide with the original ones, as in that case advection has not happened yet. For increasing t , water is advected according to our prescribed transport matrix, and some cells shift to a different biome states, according to the updated precipitation field.

List of Figures

2.1 South American precipitation, with our Amazon box, together with an exemplification of our measure of the dry season length. Panel (a) shows our Amazon box (red square) superimposed on the precipitation field for South America as in ERA5 observations. The table-top mountains mentioned in the text (Tepuis) are located in the North of the box (they correspond with the local peaks of precipitation). Panel (b) shows the daily precipitation (light green) from ERA5 observations, with a superimposed 28-days running mean (dark green). The five blue dots indicate random (example) days between the maximum and the minimum of precipitation intensity (May-August), and the red dots the first day when precipitation reaches the same value. τ indicates the time lag in days (“Precipitation recovery lag”). Panel (c) shows the length of τ depending on the prescribed onset of the dry season (position of the blue dot). The colour indicates the strength of the precipitation connected to that τ (i.e. the ordinate of the horizontal line in panel (a)). 12

3.1	Validation of different models against observations. Panel (a): Difference of selected climate models with observations. Each model is represented by a solid line, the zero line (black dashed) indicated a “perfect” model, the one that coincides with observations. A model that constantly over-/underestimates is considered to perform better, as a homogeneous over-/underestimation indicates that the model is able to properly reproduce the monthly variability of precipitation, and the scaling defined by equation 2.1 can efficaciously counteract homogeneous biases. Panel (b): Each point corresponds to a climate model, and the big square dot indicates the model spread (the position of the point is the x, y average, the errorbars are the x, y standard deviations). We took the difference between model and observation, and calculated the root mean square RMS (x-axis) and standard deviation STD (y-axis). The colour of each point indicates the time integral (discrete sum) of such difference. Note that the colorbar is not homogeneous, but bilinear. Each legend entry includes the atmospheric spatial resolution of each model.	15
3.2	Comparison between ERA5 observations and CESM1 UH PD climate model. Panel (a) shows the daily precipitation (lighter colors) with a superimposed 10-days running mean (darker colors). Panel (b) shows the time mean differences between model and observations. Panel (c) includes the comparison of the two probability density functions PDF: the histograms are the distributions of precipitation (time and space averaged); the solid lines are the means (first moment); the dotted lines are different percentiles. Panel (d) compares the dry season length with the method explained in section 2.1.2 (see caption of fig. 2.1 for further clarification): round dots refer to CESM1 UH PD values; square dots refer to ERA5 values.	16
3.3	Similar to figure 3.2 but the comparison is between CESM1 UH PD and CESM1 UH FU	18

- 4.1 Exemplification of the changes to the climatology used in sensitivity analyses. Panel (a) shows a simplified version of the changes applied in the work of section 4.1: a spatially-uniform alteration of precipitation and temperature (the latter not shown in the figure) was applied to the climatology; each line corresponds to an alteration with a different intensity; if the values were to become negative, they were substituted with zero (see “-120mm” line). Panel (b) shows the strengthening of the dry season applied to the driest four months (see section 4.3): at each step (5 in the figure) a decrease of X% is applied to the driest months, until the precipitation is zero for those months. Panel (c) shows an exemplified version of the lengthening applied in section 4.2: from the driest month until the end of the year, precipitation has been uniformly reduced; in the months where the values become lower than the original driest month, precipitation has been set to the original driest value; the blue and red dots are to indicate the beginning and end of the dry season (as defined in section 2.1.2). 20
- 4.2 Simulated response of the Amazon rainforest to spatially uniform changes of temperature and precipitation. The simulated fraction over the Amazon rainforest of dry biomes (*savanna* and *tropical xerophytic shrubland*, panel (a)) and trees (*tropical evergreen forest*, *tropical deciduous forest*, *tropical semideciduous forest* and *tropical conifer forest*, panel (b)) are plotted as contour lines. The original input values are plotted in both panels as a green dot (it corresponds to “zero changes” for precipitation and temperature). Scaled yearly inputs from CESM1 UH are plotted as square dots (present-day) and round dots (future) in both panels. Panels also include an estimation of the spread of PD and FU points: the blue and red squares are delimited by ± 1 standard deviation in both coordinates. Statistically (under the assumption of independent coordinates), 46.5% of the points fall inside the squares. 21

4.3	Simulated response of the Amazon rainforest to a lengthening of the dry season (as defined in section 4.2, and exemplified in panel (c) of figure 4.1). Precipitation was decreased after it had reached its minimum value, producing a lengthening of the dry season. Note that our measure of the length of the dry season depends on where it is defined to start: for plotting purposes it is defined to start on June 1 st (other choices would scale the x-axis). The simulated fraction over the Amazon rainforest of dry biomes (<i>savanna</i> and <i>tropical xerophytic shrubland</i>) and trees (<i>tropical evergreen forest</i> , <i>tropical deciduous forest</i> , <i>tropical semideciduous forest</i> and <i>tropical conifer forest</i>) are plotted. The black vertical dashed line is the projected lengthening of the dry season from CESM1 UH when it is defined to start on the 1 st of June.	22
4.4	Simulated response of the Amazon rainforest to a strengthening of the dry season (as defined in section 4.3, and exemplified in panel (b) of figure 4.1). Precipitation was reduced in the n driest months (y-axis) in percentage steps (x-axis). The simulated fraction over the Amazon rainforest of dry biomes (<i>savanna</i> and <i>tropical xerophytic shrubland</i> , panel (a)) and trees (<i>tropical evergreen forest</i> , <i>tropical deciduous forest</i> , <i>tropical semideciduous forest</i> and <i>tropical conifer forest</i> , panel (b)) are plotted as contour lines. White diamonds indicate the mean precipitation variation on the n driest months of each future year compared to present-day mean (from CESM1 UH). Red diamonds are the means of all the white ones.	23
4.5	Simulated biome distribution for South America (with Amazon rainforest highlighted) in present-day and future. In both panels: the red contour is the mask of the Amazon rainforest from van der Laan et al. ²² ; the colours correspond to the biomes as in the legend. Panel (a) shows the result of running BIOME4 with its original input data. Panel (b) shows the result of a run with the scaled difference between CESM1 UH FU and PD, with the method explained in equation 2.1, scaling the mean of all future years with the present-day mean.	26

4.6	Schematic representation of the implemented evaporation advection scheme. In the example, the Amazon rainforest is zonally divided in three cells. Each cell has an evaporation E_i that depends on the biome present. In each cell, precipitation equals $R_i = pE_i$, with $p < 1$. Each cell advects $ADV_{ij} = (1 - p)E_i$ to its west-neighbouring j cell. Suppose that in the initial state ($t = 0$) the three cells are as the first row of the table. At $t > 0$ cells 1 and 2 could change state due to loss of water through advection. Note that cell 1 advects out of the boundaries, thus this method does not conserve total water.	27
4.7	Results of the implementation of the evaporation advection method. Starting from the original output , the advection method was implemented across time. Panel (a) shows the biome fractions of trees and dry biomes for different values of the p parameter (y-axis), in time (x-axis). Panel (b) presents a cross-section of panel (a) at the last timestep. Thus, here the blue (trees) and red (dry biomes) lines indicate the equilibrium fractions for different p values.	28
S1	Comparison between different precipitation fields to be possibly used as BIOME4 input. Panel (a) shows the time-mean difference between the original BIOME4 input data and CESM1 UH PD. Panel (b) shows the time-mean difference between future and present-day for CESM1 UH results. Note that the original input only covers the land, while CESM1 UH has data also for the oceans: this will not affect the results because BIOME4 does not simulate atmospheric circulation, and in any case other spatial inputs are defined only on land (such as soil characteristics).	33
S2	Comparison between different temperature fields to be possibly used as BIOME4 input. Panel (a) shows the time-mean difference between the original BIOME4 input data and CESM1 UH PD. Panel (b) shows the time-mean difference between future and present-day for CESM1 UH results. Note that the original input only covers the land, while CESM1 UH has data also for the oceans: this will not affect the results because BIOME4 does not simulate atmospheric circulation, and in any case other spatial inputs are defined only on land (such as soil characteristics).	34

S3	Time averages comparison between the precipitation for present-day from all the data sources used in this work. Each panel shows the time average of one model. Each title includes the spatial resolution of the model. The non-transparent area is the one corresponding to the Amazon box (see section 2.1.2), the semi-transparent area is shown for completeness. Note that the different spatial resolution produce a different size of the non-transparent area.	35
S4	Time averages comparison between the precipitation differences between all the climate models used in this work and ERA5 observations. Each panel shows the time-mean difference of one model. The solid black contour corresponds to the Amazon box (see section 2.1.2). Note that all the models are bilinearly up-/down-scaled to match ERA5 observations.	36
S5	Simulated response of the Amazon rainforest to a change in CO ₂ concentration. CO ₂ concentration (x-axis) was increased in steps, and BIOME4 was run at each step. The simulated fraction over the Amazon rainforest of dry biomes (<i>savanna</i> and <i>tropical xerophytic shrubland</i>) and trees (<i>tropical evergreen forest</i> , <i>tropical deciduous forest</i> , <i>tropical semideciduous forest</i> and <i>tropical conifer forest</i>) are plotted, both separately and grouped. The vertical black dashed line is the CESM1 UH FU value.	37
S6	Dependency of the equilibrium states for the rainforest simulated with BIOME4 and our evaporation advection scheme on the value of the p parameter. The p parameter is indicated in the title of each panel, together with the timestep of each screenshot (all the integrations had already reached equilibrium). Colors correspond to biomes (see legend of figure 4.5). The evaporation advection method has been applied only inside the red box, the values outside are the ones of the original input of BIOME4. The results for $p = 1$ coincide with the original ones, as in that case no advection takes place. For decreasing p , the amount of water that is advected out of a gricell increases, and more cells shift to dry biomes.	38

S7 Variation of the state of the rainforest in time, as simulated with BIOME4 and our evaporation advection scheme, with a fixed p parameter. Colors correspond to biomes (see legend of figure 4.5). The evaporation advection method has been applied only inside the red box, the values outside are the ones of the original input of BIOME4. The results for $t = 0$ coincide with the original ones, as in that case advection has not happened yet. For increasing t , water is advected according to our prescribed transport matrix, and some cells shift to a different biome states, according to the updated precipitation field. 39

List of Tables

2.1	Fully-coupled climate models used in this work with their spatial resolution.	10
2.2	BIOME4 inputs description	13
2.3	BIOME4 outputs description	13
4.1	Transport matrix of advected moisture from cell C to neighbouring cells. The percentages in the cells indicate how much of the water available for advection from cell C is advected to that cell.	25

Bibliography

- [1] Chris Huntingford, Rosie A Fisher, Lina Mercado, Ben B.B Booth, Stephen Sitch, Phil P Harris, Peter M Cox, Chris D Jones, Richard A Betts, Yadvinder Malhi, Glen R Harris, Mat Collins, and Paul Moorcroft. Towards quantifying uncertainty in predictions of Amazon ‘dieback’. *Philosophical Transactions of the Royal Society B: Biological Sciences*, 363(1498):1857–1864, May 2008.
- [2] Marina Hirota, Milena Holmgren, Egbert H. Van Nes, and Marten Scheffer. Global Resilience of Tropical Forest and Savanna to Critical Transitions. *Science*, 334(6053):232–235, October 2011.
- [3] P. M. Cox, R. A. Betts, M. Collins, P. P. Harris, C. Huntingford, and C. D. Jones. Amazonian forest dieback under climate-carbon cycle projections for the 21st century. *Theoretical and Applied Climatology*, 78(1-3), June 2004.
- [4] Carlos A. Nobre, Gilvan Sampaio, Laura S. Borma, Juan Carlos Castilla-Rubio, José S. Silva, and Manoel Cardoso. Land-use and climate change risks in the Amazon and the need of a novel sustainable development paradigm. *Proceedings of the National Academy of Sciences*, 113(39):10759–10768, September 2016.
- [5] Niklas Boers, Norbert Marwan, Henrique M. J. Barbosa, and Jürgen Kurths. A deforestation-induced tipping point for the South American monsoon system. *Scientific Reports*, 7(1):41489, February 2017.
- [6] Jin-Ho Yoon and Ning Zeng. An Atlantic influence on Amazon rainfall. *Climate Dynamics*, 34(2-3):249–264, February 2010.
- [7] Eric A. Davidson, Alessandro C. de Araújo, Paulo Artaxo, Jennifer K. Balch, I. Foster Brown, Mercedes M. C. Bustamante, Michael T. Coe, Ruth S. DeFries, Michael Keller, Marcos Longo, J. William Munger, Wilfrid Schroeder, Britaldo S. Soares-Filho, Carlos M. Souza, and Steven C. Wofsy. The Amazon basin in transition. *Nature*, 481(7381):321–328, January 2012.

- [8] M. Gloor, R. J. W. Brienen, D. Galbraith, T. R. Feldpausch, J. Schöngart, J.-L. Guyot, J. C. Espinoza, J. Lloyd, and O. L. Phillips. Intensification of the Amazon hydrological cycle over the last two decades. *Geophysical Research Letters*, 40(9):1729–1733, May 2013.
- [9] Celso H. L. Silva Junior, Ana C. M. Pessôa, Nathália S. Carvalho, João B. C. Reis, Liana O. Anderson, and Luiz E. O. C. Aragão. The Brazilian Amazon deforestation rate in 2020 is the greatest of the decade. *Nature Ecology & Evolution*, 5(2):144–145, February 2021.
- [10] Luis Fernando Salazar and Carlos A. Nobre. Climate change and thresholds of biome shifts in Amazonia: CLIMATE CHANGE AND AMAZON BIOME SHIFTS. *Geophysical Research Letters*, 37(17):n/a–n/a, September 2010.
- [11] Phil P Harris, Chris Huntingford, and Peter M Cox. Amazon Basin climate under global warming: the role of the sea surface temperature. *Philosophical Transactions of the Royal Society B: Biological Sciences*, 363(1498):1753–1759, May 2008.
- [12] Chris A. Boulton, Peter Good, and Timothy M. Lenton. Early warning signals of simulated Amazon rainforest dieback. *Theoretical Ecology*, 6(3):373–384, August 2013.
- [13] L. C. Jackson, R. Kahana, T. Graham, M. A. Ringer, T. Woollings, J. V. Mecking, and R. A. Wood. Global and European climate impacts of a slowdown of the AMOC in a high resolution GCM. *Climate Dynamics*, 45(11-12):3299–3316, December 2015.
- [14] Marcos Daisuke Oyama and Carlos Afonso Nobre. A new climate-vegetation equilibrium state for Tropical South America: A NEW CLIMATE-VEGETATION STATE. *Geophysical Research Letters*, 30(23):n/a–n/a, December 2003.
- [15] Kerry H. Cook and Edward K. Vizy. Effects of Twenty-First-Century Climate Change on the Amazon Rain Forest. *Journal of Climate*, 21(3):542–560, February 2008.
- [16] Angela Cheska Siongco, Cathy Hohenegger, and Bjorn Stevens. The Atlantic ITCZ bias in CMIP5 models. *Climate Dynamics*, 45(5-6):1169–1180, September 2015.
- [17] Antonios Mamalakis, James T. Randerson, Jin-Yi Yu, Michael S. Pritchard, Gudrun Magnusdottir, Padhraic Smyth, Paul A. Levine, Sungduk Yu, and Efi Foufoula-Georgiou. Zonally contrasting shifts of the tropical rain belt in response to climate change. *Nature Climate Change*, 11(2):143–151, February 2021.

- [18] André Jüling, Anna von der Heydt, and Henk A. Dijkstra. Effects of strongly eddying oceans on multidecadal climate variability in the Community Earth System Model. *Ocean Science*, 17(5):1251–1271, September 2021.
- [19] Gilvan Sampaio, Carlos Nobre, Marcos Heil Costa, Prakki Satyamurty, Britaldo Silveira Soares-Filho, and Manoel Cardoso. Regional climate change over eastern Amazonia caused by pasture and soybean cropland expansion. *Geophysical Research Letters*, 34(17):L17709, September 2007.
- [20] Marcos Heil Costa and Gabrielle Ferreira Pires. Effects of Amazon and Central Brazil deforestation scenarios on the duration of the dry season in the arc of deforestation: AMAZON DEFORESTATION SCENARIOS AND THE DURATION OF THE DRY SEASON. *International Journal of Climatology*, 30(13):1970–1979, November 2010.
- [21] Jed O Kaplan. Geophysical Applications of Vegetation Modeling. page 129.
- [22] I. T. van der Laan-Luijkx, I. R. van der Velde, M. C. Krol, L. V. Gatti, L. G. Domingues, C. S. C. Correia, J. B. Miller, M. Gloor, T. T. van Leeuwen, J. W. Kaiser, C. Wiedinmyer, S. Basu, C. Clerbaux, and W. Peters. Response of the Amazon carbon balance to the 2010 drought derived with CarbonTracker South America: AMAZON CARBON CYCLE DURING 2010 DROUGHT. *Global Biogeochemical Cycles*, 29(7):1092–1108, July 2015.
- [23] Arie Staal, Obbe A Tuinenburg, Joyce HC Bosmans, Milena Holmgren, Egbert H van Nes, Marten Scheffer, Delphine Clara Zemp, and Stefan C Dekker. Forest-rainfall cascades buffer against drought across the amazon. *Nature Climate Change*, 8(6):539–543, 2018.